Condensed Matter Physics. Polymer Physics

UDC 538.9+537.3 DOI: 10.33910/2687-153X-2020-1-4-135-141

Molecular mobility in crystallising aromatic thermoplastic polyimide R-BAPS

N. A. Nikonorova✉[1], A. A. Kononov[2], R. A. Castro Arata[2]

[1] Institute of Macromolecular Compounds of Russian Academy of Sciences,
31 Bolshoy Ave., Saint Petersburg 199004, Russia
[2] Herzen State Pedagogical University of Russia, 48 Moika Emb., Saint Petersburg 191186, Russia

Authors

Natalia A. Nikonorova, ORCID: 0000-0002-7928-9227, e-mail: n_nikonorova2004@mail.ru

Alexey A. Kononov, ORCID: 0000-0002-5553-3782

Rene Alejandro Castro Arata, ORCID: 0000-0002-1902-5801

For citation: Nikonorova, N. A., Kononov, A. A., Castro Arata, R. A. (2020) Molecular mobility in crystallising aromatic thermoplastic polyimide R-BAPS. *Physics of Complex Systems*, 1 (4), 135–141. DOI: 10.33910/2687-153X-2020-1-4-135-141

Received 27 May 2020; reviewed 11 June 2020; accepted 11 June 2020.

Abstract. The molecular mobility of the thermoplastic aromatic *R-BAPS* polyimide films *based on 1,3-bis (3,3'-4,4'-dicarboxyphenoxy) benzene (dianhydride) and 4,4'-bis (4-aminophenoxy) biphenyl* was studied using the dielectric method. Two relaxation regions of dipole polarisation caused by local mobility of phenylene groups in the diamine (γ process) and in the diamine and dianhydride macromolecule parts (β process) were identified in the glassy state, In the high-elastic state, two relaxation processes, α and α_{MWS}, were also observed. The α process is due to the large-scale segmental mobility of macromolecules. The α_{MWS} process is caused by the relaxation at the boundary between amorphous and crystalline regions, i.e., the Maxwell-Wagner-Sillars relaxation. Moreover, a structural transition due to melting was observed in the initial samples.

Keywords: thermoplastic aromatic polyimide, molecular mobility, dielectric spectroscopy, relaxation time, glass transition temperature.

Introduction

Nowadays, well-developed synthesis methods make it possible to obtain polyimides (PI) with a very diverse chemical structure and molecular architecture and, consequently, with largely varied physical properties (Bryant 2002; Sroog 1969). There is a correlation between the polymer physical properties and the molecular mobility of the polar kinetic units. One of the methods to identify this correlation is dielectric spectroscopy. When the polymer system is studied by the dielectric method, the polar groups ("labels") reorientation causes the temperature-frequency dependences of the dielectric absorption regions. This provides information on the polymer molecular mobility at all molecular organisation levels. In turn, molecular motion properties depend on inter- and intramolecular interactions determined by the polymer chemical structure and morphological features (Hedvig 1977; Riande, Diaz-Calleja 2004). At least three relaxation regions of dipole polarisation—the γ, β and α processes—were detected using the dielectric spectroscopy for PIs with a largely varied chemical structure (Cheng et al. 1995; Chisca et al. 2011; Jacobs et al. 2010; Sun et al. 1992).

The research aim is to analyse the dielectric relaxation processes in the R-BAPS aromatic polyimide as well as to determine the molecular mobility mechanisms that cause dipole polarisation relaxations.

Experimental methods

The samples were thermoplastic polyimide films based on 1,3-bis- (3,3'-4,4'-dicarboxyphenoxy) benzene and 4,4'-bis- (4-aminophenoxy) biphenyl (R-BAPS) (Fig. 1) synthesised at the Institute

of Macromolecular Compounds, Russian Academy of Sciences (Smirnova et al. 2013; Svetlichnyi, Kudryavtsev 2003).

R-BAPS films were obtained from the 20% polyamide acid (PAA) solution, molecular weight Mw ~30,000 g/mol, dried at 60°C for 24 hours and subjected to stepwise heat treatment for 1 hour at 100°C, 200°C and 300°C (Kamalov et al. 2020; Yudin et al. 2002).

The dielectric spectra (frequency dependences of the dielectric loss factor, $\varepsilon'' = \phi(f)$) were obtained in the frequency range 10^{-1}–$3 \cdot 10^6$ Hz and temperatures –100–+400°C using the "Concept-21" broadband dielectric spectrometer (Novocontrol Technologies GmbH) with an ALPHA-ANB high-resolution automatic frequency analyser. The ~25–40 μm films were pressed between brass electrodes (the upper electrode was 20 mm in diameter) at a ~30°C higher temperature than the glass transition temperature. For the first measurement, the films were additionally warmed up to 250°C (the initial samples).

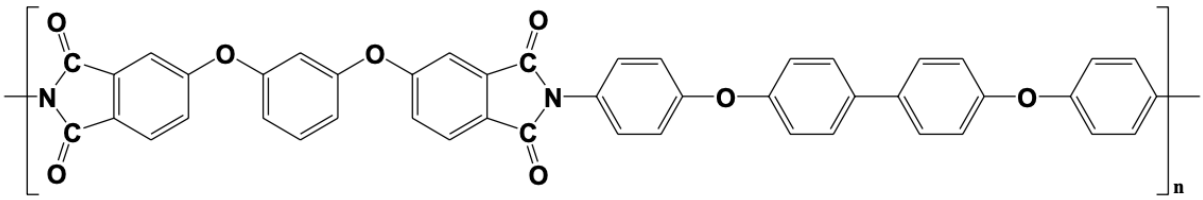

Fig. 1. The R-BAPS chemical formula

R-BAPS dielectric behaviour

The dielectric behaviour in the entire temperature range is shown in Fig. 2 which presents the temperature dependences of $tg\delta = \phi(T)$ for R-BAPS (for the initial sample) at various frequencies. Fig. 2 shows three $tg\delta_{max}$ regions: γ and β (in a glassy state) and α (in a highly elastic state) caused by the relaxation processes of the dipole polarisation, since the maximum temperature shifts towards high temperatures as frequency increases. A sharp increase in the dielectric loss and $tg\delta_{max}$ region due to the conductivity process was observed at temperatures exceeding the α process. Moreover, at 320°C there was a tgδ peak; the temperature did not change with frequency, while the intensity sharply decreased with frequency. This dielectric behaviour pattern is characteristic of a structural (non-relaxation) transition caused, in particular, by melting, which is confirmed by the DSC data (Kamalov et al. 2020). The tgδ peak at 320°C indicates a certain crystallinity of the initial sample. Heating the sample to 340°C (above the melting temperature) suppresses the structural transition at 320°C, as can be seen in the inset (Fig. 2).

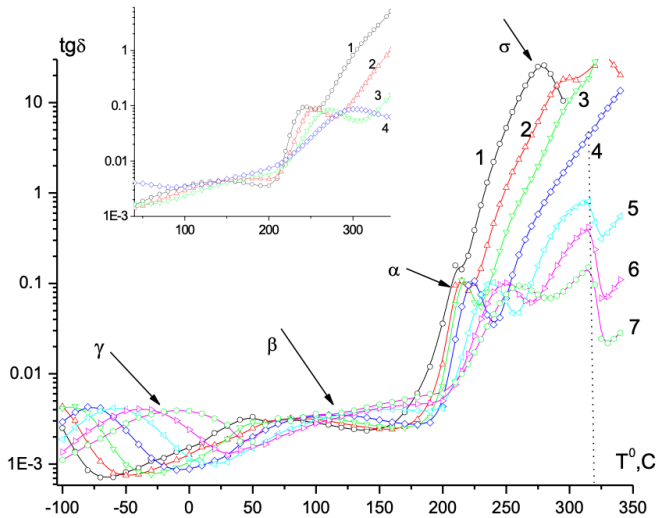

Fig. 2. The tgδ temperature dependences for R-BAPS at frequencies 0.1 (1), 1 (2), 10 (3), 100 (4), 1000 (5), 10000 (6) and 100000 (7) Hz, the initial measurement and the measurement after warming up to 340°C (inset)

DOI: 10.33910/2687-153X-2020-1-4-135-141

The dielectric spectra were analysed by describing the complex dielectric constant ε^* using the empirical Havriliak-Negami equation (HN), which, as a rule, reliably describes the dependences $\varepsilon'' = \phi(f)$ for various relaxation processes (Havriliak, Negami 1967):

$$\varepsilon^*(\omega) - \varepsilon_\infty = \sum_{k=1}^{n} \mathrm{Im}\left[\frac{\Delta\varepsilon_k}{\{1+(i\omega\tau_{HN_k})^{\alpha_k}\}^{\beta_k}}\right], \quad (1)$$

where $\varepsilon^* = \varepsilon'(\omega) - i\varepsilon''(\omega)$; $\omega = 2\pi f$ is the angular frequency; $\Delta\varepsilon = \varepsilon_0 - \varepsilon_\infty$ is the increment of the dielectric permittivity; τ_{HN} is the characteristic Havriliak-Negami relaxation time; α_{HN} and β_{HN} are the calculated parameters corresponding to the expansion and asymmetries of the relaxation time distribution, respectively, k is the number of the relaxation processes.

Above T_g, the contribution due to conductivity was taken into account in the formula (1): $\frac{\sigma_{dc} a}{\varepsilon_v \omega^s}$, where σ_{dc} is the direct current electrical conductivity, a is the constant, ε_v is the dielectric constant of the vacuum (Vallerien et al. 1989); τ_{max} was calculated by the following formula (Diaz-Calleja 2000):

$$\tau_{max} = \tau_{HN}\left[\frac{\sin\left(\frac{\pi(\alpha_{HN})\beta_{HN}}{2(\beta_{HN}+1)}\right)}{\sin\left(\frac{\pi(\alpha_{HN})}{2(\beta_{HN}+1)}\right)}\right]^{1/(\alpha_{HN})} \quad (2)$$

Fig. 3 shows the dielectric spectra for R-BAPS at various temperatures in the γ and β process regions, which are reliably described by a single HN process.

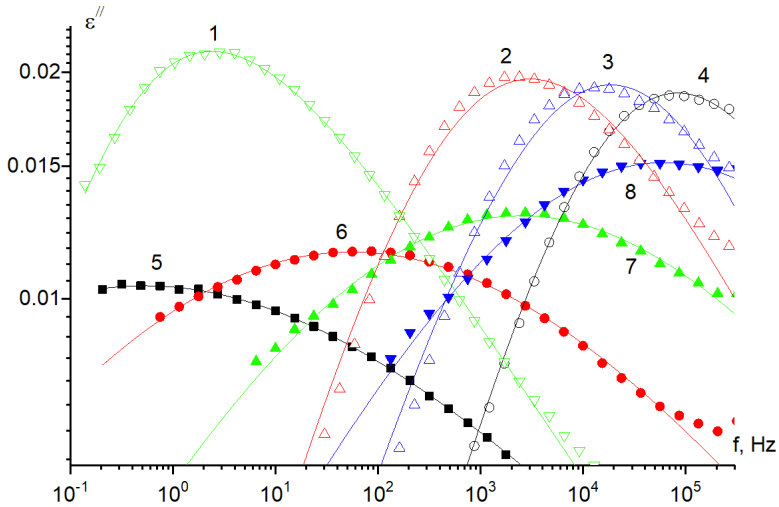

Fig. 3. The ε'' frequency dependences in the γ (1–4) and β (5–8) process regions for R-BAPS at –100°C (1), –80°C (2), –60°C (3), –10 °C (4), 60°C (5), 100°C (6), 140°C (7) and 180°C (8).
Symbols are experimental points. Continuous lines are the calculation according to the HN formula

In the highly elastic state, the polymer dielectric spectroscopy is usually described by the sum of two components—the α process and the contribution to the dielectric loss due to conductivity. In the case of the initial R-BAPS sample, the dielectric spectra in the 230–320°C temperature range can be described as the sum of three components: the α and α_{MWS} (at lower frequencies) relaxation processes and the contribution due to conductivity. Fig. 4 shows several dielectric spectra in a highly elastic state and a spectrum separation into three components.

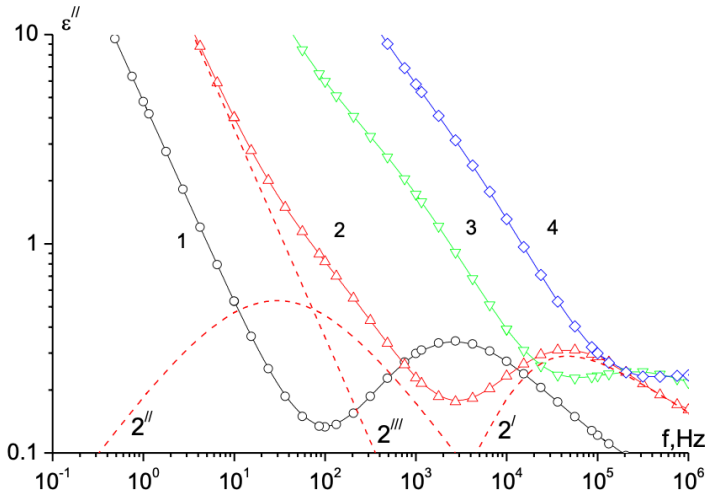

Fig. 4. The ε'' frequency dependences in the α and αMWS relaxation process regions for R-BAPS (the initial sample) at 240°C (1), 260°C (2), 280°C (3) and 300°C (4). Symbols are experimental points. Continuous lines are the description according to the HN formula. The dashed lines are the dielectric spectrum separation at 260°C into the α ($2'$) and αMWS processes ($2''$) and the contribution due to conductivity ($2'''$) according to the HN formula.

Despite the fact that the α_{MWS} process shows only a slight deviation from the linear increase in ε'' in the low frequencies / high temperatures (LF/HT) range, its allocation from the spectrum according to the HN formula is quite reliable, as shown in Fig. 5 (ε'' losses due to the conductivity are subtracted).

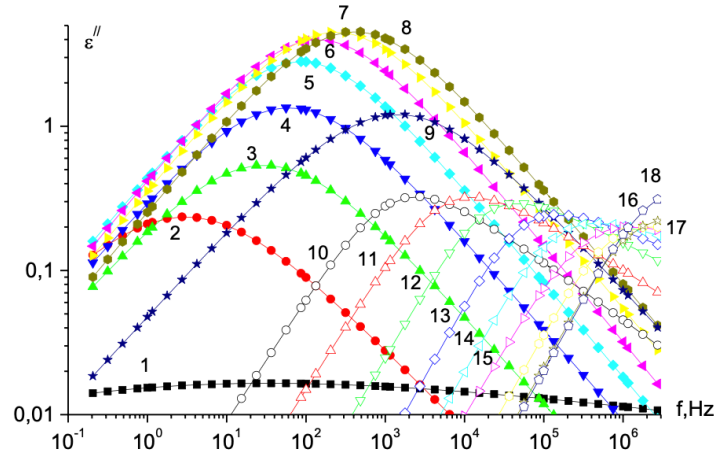

Fig. 5. The ε'' frequency dependences in the αMWS (1–9) and α (10–18) process regions for R-BAPS (the initial sample) at 240°C (1.10), 250°C (2.11), 260°C (3.12), 270°C (4.13), 280°C (5.14), 290°C (6.15), 300°C (7.16), 310°C (8.17) and 320°C (9.18)

The τ_{max} values calculated by the HN formula for R-BAPS (the initial sample) in the γ, β, α and α_{MWS} process regions are shown in Fig. 6, curves 1, 2, 3 and 5, respectively. After heating above 340°C, the relaxation region corresponding to the α_{MWS} process (curve 4) disappears; however, the relaxation time in the regions corresponding to the γ, β and α processes does not change.

For the γ, β and α_{MWS} processes, the $-log\tau_{max}$ dependencies on the inverse temperature are linear and are described by the Arrhenius equation:

$$\tau(T)_{max} = \tau_0 \exp\left(\frac{E_a}{RT}\right), \quad (3)$$

where $\tau_0 = \tau_{max}$ at $T \to \infty$, E_a is the activation energy, R is the universal gas constant.

DOI: 10.33910/2687-153X-2020-1-4-135-141

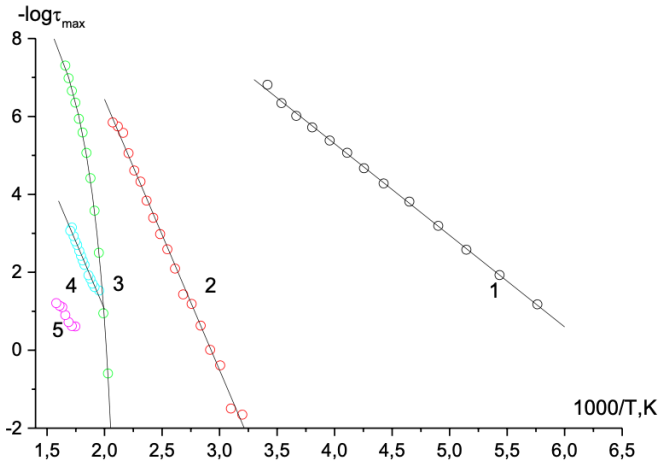

Fig. 6. The $-\log\tau_{max}$ dependencies on the inverse temperature for R-BAPS (the initial sample) for the γ (1), β (2), α (3), αMWS (4) and SCP (5) processes. τmax points are calculated using the HN formula. Curves describe the dependencies according to the formulas 3 (1, 2 and 5) and 4 (3)

The linear dependence $-log\tau_{max} = \phi(1/T)$ indicates that the activation energy does not depend on the temperature.

For the α process, the dependence $-log\tau_{max} = \phi(1/T)$ is curvilinear and is well described by the empirical Vogel-Tammann-Hesse (F-T-H) equation, which describes relaxation processes where the activation energy depends on the temperature (Donth 2001; Vogel 1921):

$$\tau_{max} = \tau_0 \exp(\frac{B}{T - T_0}) \quad (4),$$

where τ_0, B and T_0 are calculated parameters that do not depend on temperature (τ_0 is the pre-exponential factor, B is the activation parameter and T_0 is the so-called Vogel temperature).

Molecular mechanisms of dielectric processes

Three relaxation processes—the γ and β processes in the glassy state and the α process in the highly elastic state—were found for R-BAPS as well as for the previously studied PIs with different chemical structure (Cheng et al. 1995; Chisca et al. 2011; Jacobs et al. 2010; Nikonorova et al. 2019; Sun et al. 1992). Molecular mechanisms were proposed for the γ, β and α processes. It was believed that the γ process is caused by the local mobility of phenyl rings in the diamine part of the macromolecule as well as by the mobility of the bound water molecules (Chisca et al. 2011; Jacob et al. 2010). For the γ process, the relaxation time did not depend on the polymer structure, and the temperature $tg\delta_{max}$ was ~–100°C (at 1 Hz). For R-BAPS, the molecular source of the γ process is reorientation of the phenyl rings with the adjacent ether groups; therefore, the temperature $tg\delta_{max}$ was ~–100°C (at 1 Hz). The equation (3) parameters are given in Table 1.

Table 1. Parameters of equation 3 for γ, β and αMWS processes

	γ	β	α_{MWS}
$-lg\tau_0$	14.7	20.34	14.95
E_a, kcal/mol	10.8	10.8	31.9

It was suggested that the molecular mechanism of the β process corresponds to mobility in the dianhydride macromolecule part (Chisca et al. 2011), rotation of the para-phenylene units in the diamine part (Sun et al. 1992) and correlated local movements in both macromolecule parts (Chisca et al. 2011;

Jacobs et al. 2010; Sun et al. 1992). For the β process, the relaxation time depended on the sample chemical structure, thermal treatment and morphology, and the temperature $tg\delta_{max}$ was in the 50–150°C range (at 1 Hz). Based on the R-BAPS chemical structure, it can be assumed that the β process is related to the local movements of the phenyl rings in the diamine and dianhydride macromolecule parts with the adjacent ether and amide polar groups. In other words, the β process is the superposition of several molecular mobility modes with close relaxation times that cannot be separated. For R-BAPS, the temperature $tg\delta_{max}$ in the β process region was ~+75°C (at 1 Hz). The equation (3) parameters for the β process are given in Table 1.

The molecular source of the α process is the cooperative large-scale segmental mobility of a macromolecule related to the transition from the glassy to the highly elastic state. In this case, the temperature dependence $-\log\tau_{max}$ is usually nonlinear and the apparent activation energy varies depending on the temperature. In the α process region, the dependence $-\log\tau_{max} = \phi(1/T)$ separates the glassy state region (on the right) from the highly elastic state region (on the left). The equation (4) parameters $-\log\tau_0$, B and T_0 for the α process are 11.6 s, 1564 and 421 K, respectively. For R-BAPS, the temperature dependence of the relaxation time is shown by curve 3. The glass transition temperature of R-BAPS is 222°C. T_g was determined using the conventional dielectric method procedure—extrapolation of the $-\log\tau_{max} = \phi(1/T)$ dependence described by the F-T-H equation $\log\tau_{max} = 0$ ($\tau_{max} = 1$ s).

In polymers, a rapid increase in the dielectric loss is typically observed at temperatures above the α transition (in the highly elastic state) at HT / LF due to the space-charge polarisation (SCP). The SCP molecular source is the charges block on the electrode / sample surface which forms a double electric layer with large capacity that demonstrates huge values of ε', ε'' and tgδ. Moreover, the increment values of the dielectric permittivity (Δε) reach ~100...10 000 (Chisca et al. 2011; Lu et al. 2006; Neagu et al. 2000; Samet et al. 2015). The SCP effects are largely determined by the polymer purity (uncontrolled impurities, residual solvents and starting destruction of macromolecules in the polymer), rather than its chemical structure. Space-charge polarisation is considered a "parasitic" effect. During the polymer examination by the dielectric method, measures are taken to reduce it. The SCP temperature-frequency coordinates for R-BAPS are shown by curve 5 in Fig. 6, which is typical for this effect (Neagu et al. 2000; Samet et al. 2015).

Along with the SCP effect, polymers with heterogeneous structure—such as polymer mixtures, two-three-phase systems, nanocomposites and crystallising polymers—at HT / LF can demonstrate the Maxwell-Wagner-Sillars (MWS) polarisation, where the $-\log\tau_{max} = \phi(1/T)$ temperature dependence lies between the α process and the SCP effect (Chisca et al. 2011; Hedvig 1977; Klonos et al. 2017; Lu et al. 2006; Neagu et al. 2000; Samet et al. 2015; Tsonos et al. 2001). The MWS polarisation arises due to polarisation at the phase boundary when microphases of such systems have different conductivity and permittivity values. For R-BAPS, the α_{MWS} relaxation process, which is between the α process and the SCP effect, demonstrates several features. Firstly, this process takes place in the interval from T_g up to the melting temperature. Above 320°C it disappears, while the α process can be observed up to 350°C. Secondly, the Δε values of the α_{MWS} process are ~7–12. Thirdly, the $\lg\tau_{max} = \phi(1/T)$ dependence is linear (Fig, 6, curve 4, equation 3 parameters are given in the table), which is typical for the MWS polarisation (Klonos et al. 2017; Tsonos et al. 2001). These features suggest that the α_{MWS} relaxation process is caused precisely by the Maxwell-Wagner-Sillars polarisation in the initial P-BAPS samples where melting is observed. The molecular mechanism of the α_{MWS} process in R-BAPS is polarisation according to the MWS type at the boundary between the amorphous and the crystalline phases of the sample. This α_{MWS} process is observed only in crystallising samples and disappears in the amorphous sample after heating above 320°C. Annealing at 280°C, at which the R-BAPS crystalline phase is formed (Smirnova et al. 2013), causes the α_{MWS} process to reappear, i.e. this process is reproducible.

Conclusion

Thus, several relaxation regions of dipole polarisation, typical of the dielectric absorption pattern demonstrated by PIs with different structure, were identified by the dielectric method for aromatic thermoplastic PI R-BAPS in the –100–350°C temperature range. The dielectric spectra showed three maximum regions; these regions listed in order of increasing temperature are caused by local mobility in the diamine (the γ process) and joint movement in the diamine and dianhydride macromolecule parts (the β process), as well as the segmental cooperative mobility of macromolecules (the α process),

 DOI: 10.33910/2687-153X-2020-1-4-135-141

correspondingly. In a partially crystallised sample at temperatures exceeding the α process (at HT / LF), it was possible to see the α_{MWS} process which reflects the polarisation at the interface between the amorphous and crystalline phases, i.e., the MWS type polarisation. The difference in the sample dielectric behaviour is that in addition to the γ, β and α processes observed in the amorphous sample (warmed above 320°C), the partially crystalline (initial) sample also demonstrates the α_{MWS} process.

References

Bryant, R. G. (2002) Polyimides. In: H. F. Mark (ed.). *Encyclopedia of polymer science and technology. Vol. 7*. 4th ed. New York: John Wiley & Sons Publ., pp. 529–555. DOI: 10.1002/0471440264.pst272 (In English)

Cheng, S. Z. D., Chalmers, T. M., Gu, Y. et al. (1995) Relaxation processes and molecular motion in a new semicrystalline polyimide. *Macromolecular Chemistry and Physics*, 196 (5), 1439–1451. DOI: 10.1002/macp.1995.021960507 (In English)

Chisca, S., Musteata, V. E., Sava, I., Bruma, M. (2011) Dielectric behavior of some aromatic polyimide films. *European Polymer Journal*, 47 (5), 1186–1197. DOI: 10.1016/j.eurpolymj.2011.01.008 (In English)

Diaz-Calleja, R. (2000) Comment on the maximum in the loss permittivity for the Havriliak–Negami equation. *Macromolecules*, 33 (24), 8924–8924. DOI: 10.1021/ma991082i (In English)

Donth, E. (2001) *The glass transition: Relaxation dynamics in liquids and disordered materials. Vol. 48*. Berlin: Springer Science & Business Media Publ., 418 p. (In English)

Havriliak, S., Negami, S. (1967) A complex plane representation of dielectric and mechanical relaxation processes in some polymers. *Polymer*, 8, 161–210. DOI: 10.1016/0032-3861(67)90021-3 (In English)

Hedvig, P. (1977) *Dielectric spectroscopy of polymers*. Budapest: Akademiai Kiado, 312 p. (In English)

Jacobs, J. D., Arlen, M. J., Wang, D. H. et al. (2010) Dielectric characteristics of polyimide CP2. *Polymer*, 51 (14), 3139–3146. DOI: 10.1016/j.polymer.2010.04.072 (In English)

Kamalov, A. M., Borisova, M. E., Didenko, A. L. et al. (2020) Relaxation behavior of thermoplastic polyimide R-BAPB in the amorphous state. *Polymer Science. Series A*, 62 (2), 107–115. DOI: 10.1134/S0965545X20010058 (In English)

Klonos, P., Kyritsis, A., Bokobza, L. et al. (2017) Interfacial effects in PDMS/titania nanocomposites studied by thermal and dielectric techniques. *Colloids and Surfaces A: Physicochemical and Engineering Aspects*, 519, 212–222. DOI: 10.1016/j.colsurfa.2016.04.020 (In English)

Lu, H., Zhang, X., Zhang, H. (2006) Influence of the relaxation of Maxwell-Wagner-Sillars polarization and dc conductivity on the dielectric behaviors of nylon 1010. *Journal of Applied Physics*, 100 (5), article 054104. DOI: 10.1063/1.2336494 (In English)

Neagu, E., Pissis, P., Apekis, L. (2000) Electrical conductivity effects in polyethylene terephthalate films. *Journal of Applied Physics*, 87 (6), 2914–2922. DOI: 10.1063/1.372277 (In English)

Nikonorova, N. A., Kononov, A. A., Dao, H. T., Castro, R. A. (2019) Molecular mobility of thermoplastic aromatic polyimides studied by dielectric spectroscopy. *Journal of Non-Crystalline Solids*, 511, 109–114. DOI: 10.1016/j.jnoncrysol.2018.12.032 (In English)

Riande, E., Diaz-Calleja, R. (2004) *Electrical properties of polymers*. New York: Marcel Dekker Publ., 630 p. (In English)

Samet, M., Levchenko, V., Boiteux, G. et al. (2015) Electrode polarization vs. Maxwell-Wagner-Sillars interfacial polarization in dielectric spectra of materials: Characteristic frequencies and scaling laws. *The Journal of Chemical Physics*, 142 (19), article 194703. DOI: 10.1063/1.4919877 (In English)

Smirnova, V. E., Gofman, I. V., Ivan'kova, E. M. et al. (2013) Effect of single-walled carbon nanotubes and carbon nanofibers on the structure and mechanical properties of thermoplastic polyimide matrix films. *Polymer Science. Series A*, 55 (4), 268–278. DOI: 10.1134/S0965545X1304007X (In English)

Sroog, C. E. (1969) Polyimides. In: H. F. Mark, N. G. Gaylord, N. M. Bikales (eds.). *Encyclopedia of polymer science and technology. Vol. 11*. 1st ed. New York: John Wiley & Sons Publ., pp. 247–272. (In English)

Sun, Z., Dong, L., Zhuang, Y. et al. (1992) Beta relaxation in polyimides. *Polymer*, 33 (22), 4728–4731. DOI: 10.1016/0032-3861(92)90684-O (In English)

Svetlichnyi, V. M., Kudryavtsev, V. V. (2003) Polyimides and the problems of designing advanced structural composite materials. *Polymer Science. Series B*, 45 (5-6), 140–185. (In English)

Tsonos, C., Apekis, L., Viras, K. et al. (2001) Electrical and dielectric behavior in blends of polyurethane-based ionomers. *Solid State Ionics*, 143 (2), 229–249. DOI: 10.1016/S0167-2738(01)00858-X (In English)

Yudin, V. E., Svetlichnyi, V. M., Gubanova, G. N. et al. (2002) Semicrystalline polyimide matrices for composites: Crystallization and properties. *Journal of Applied Polymer Science*, 83 (13), 2873–2882. DOI: 10.1002/app.10277 (In English)

Vallerien, S. U., Kremer, F., Boeffel, C. (1989) Broadband dielectric spectroscopy on side group liquid crystal polymers. *Liquid Crystals*, 4 (1), 79–86. DOI: 10.1080/02678298908028960 (In English)

Vogel, H. (1921) The law of the relation between the viscosity of liquids and the temperature. *Physikalische Zeitschrift*, 22, 645–646. (In English)